Green Phosphorescent Zn(II) Halide Complexes with N,N,N′,N′-tetramethyl-P-indol-1-ylphosphonic Diamide as Ligand

Valentina Ferraro,*[a, b] Filippo Baggio,[a] Jesús Castro,[c] and Marco Bortoluzzi[a, b]

Tetrahedral Zn(II) complexes having general formula [ZnX$_2${O=P-(NMe$_2$)$_2$Ind}$_2$] (X = Cl, Br, I, NCS) were isolated from the reaction between the indol-1-yl substituted phosphoramide N,N,N′,N′-tetramethyl-P-indol-1-ylphosphonic diamide O=P(NMe$_2$)$_2$Ind and anhydrous Zn(II) precursors under mild conditions. The structures of the three halide derivatives were ascertained by single-crystal X-ray diffraction. The bromo- and iodo-derivatives revealed to be appreciably luminescent in the green region upon excitation with light below 300 nm, with emission bands centred between 520 and 530 nm. The large Stokes shifts and the excited state lifetimes in the milliseconds range indicated that triplet excited states are involved in the emission. TD-DFT calculations indicated that the luminescence is related to a ligand-centred transition with the involvement of triplet states.

Introduction

In the perspective of sustainability, luminescent earth-abundant metal complexes are of paramount importance for applications such as solar energy conversion[1] and OLED (organic light emitting diode) technology.[2] Systems based on transition metal elements such as ruthenium(II), iridium(III) or platinum(II), together with rare earths were deeply exploited for electroluminescent devices and photocatalysis.[3] However, because of their shortage, expensiveness and toxicity, the attention was moved in the last years towards more abundant elements. Among all, promising results in this field were achieved with metal centres such as manganese(II) and copper(I).[4]

Much less attention was actually devoted to zinc(II) derivatives, probably because the poor accessibility of higher oxidation states forbids luminescent mechanisms related to metal-to-ligand charge transfer. The luminescence of the majority of zinc(II) complexes reported is actually related to the fluorescence of the ligands, enhanced by coordination to the metal centre.[5] In few cases, emissions related to thermally activated delayed fluorescence (TADF) is however observable.[6]

The first application of zinc(II) derivatives as emitters for OLEDs dates back to 2000, when Sano et al. reported the application of complexes having general formula Znq$_2$ (q = 8-hydroxyquinolinate), Zn(2AZM-Me)$_2$ (2AZM-Me = conjugate base of N-methyl salicylimine), Zn(1AZM-Hex) (1AZM-Hex = conjugate base of N,N′-disalicylidenehexane-1,6-diamine) and Zn(BTZ)$_2$ (BTZ = 2-(2-benzothiazolyl)phenate).[7] The nature of the emission makes zinc(II) complexes appealing to be applied as hosts or electron-transport layers in OLEDs. For instance, the previously mentioned Zn(BTZ)$_2$ was efficiently exploited as host for 5,6,11,12-tetraphenylnaphthacene (rubrene) for the preparation of white OLED devices. The choice of the complex relies on to the good overlap existing between the emission of the zinc(II) complex and the absorption of the organic chromophore, enabling a host-to-guest Förster energy transfer.[8]

Despite being much less common, phosphorescence from zinc(II) complexes is observable when low lying s and p orbitals of the metal centre are involved in charge transfer mechanisms. Moreover, also antibonding σ* molecular orbitals with d-component from Zn(II) can be involved in emitting excited states, with mechanisms in between ligand-to-metal (LMCT) and ligand-to-ligand (LLCT) change transfer.[9] The first example of blue-phosphorescent complex was reported by Wang and co-workers using diphenyl-6,6′-dimethyl-2,2′-bipyrimidine as chelating ligand. The unusual radiative decay was evidenced by lifetimes in the μs range detected in methanol solution.[10]

Most of the luminescent zinc(II) complexes actually reported have N-donor heterocycles and O-donors derived from phenate moieties in the coordination sphere. [O=P]-donor ligands such as phosphine oxides, phosphoramides and related species were poorly investigated, despite the promising results recently achieved with other metal centres, Mn(II) in particular.[11] The literature outcomes are limited to the use of triphenylphosphine oxide,[12] but no luminescent study on the corresponding Zn(II) complexes was ever described. It is however worth noting that [ZnCl$_2$(O=PPh$_3$)$_2$] exhibited non-linear optical properties.[13] For what concerns phosphoramide Zn(II) complexes, some

[a] V. Ferraro, F. Baggio, Prof. M. Bortoluzzi
Dipartimento di Scienze Molecolari e Nanosistemi
Università Ca′ Foscari Venezia
Via Torino 155, 30170 Mestre (VE), Italy
E-mail: valentina.ferraro@unive.it
https://www.unive.it/data/persone/22949267
[b] V. Ferraro, Prof. M. Bortoluzzi
Consorzio Interuniversitario Reattività Chimica e Catalisi (CIRCC)
Via Celso Ulpiani 27, 70126 Bari, Italy
[c] Prof. J. Castro
Departamento de Química Inorgánica,
Universidade de Vigo, Facultade de Química,
Edificio de Ciencias Experimentais
36310 Vigo, Galicia, Spain
Supporting information for this article is available on the WWW under https://doi.org/10.1002/ejic.202200119
Part of the Institute Feature highlighting the "Interuniversity Consortium in Chemical Reactivity and Catalysis (CIRCC)".

tetrahedral homoleptic complexes were isolated.[14] Hexamethylphosphoramide is present in the coordination sphere of a dinuclear zinc(II) alkoxide-phenoxide-ketoiminate complex[15] and the interactions in solution of zinc(II) halides and perchlorate and of tetraphenylporphirinatozinc with hexamethylphosphoramide were investigated.[16] In the framework of our interest on luminescent first-row d[10] metal complexes for advanced technology,[17] we investigated the effects of the coordination of the previously reported *N,N,N′,N′*-tetramethyl-*P*-indol-1-ylphosphonic diamide O=P(NMe$_2$)$_2$Ind to zinc(II) precursors. Herein we report the synthesis and characterization of complexes having general formula [ZnX$_2${O=P(NMe$_2$)$_2$Ind}$_2$] (X = Cl, Br, I, NCS). The structures of the halide derivatives were ascertained by single-crystal X-ray diffraction. The bright green photoluminescence of the bromo- and iodo-complexes was investigated in detail and compared to the photoluminescence exhibited by [ZnBr$_2$(O=PPh$_3$)$_2$].

Results and Discussion

Synthesis and Characterization of the Complexes

The reaction of O=P(NMe$_2$)$_2$Ind with anhydrous ZnX$_2$ (X = Cl, Br, I, NCS) in ethanol under mild conditions afforded the corresponding neutral complexes [ZnX$_2${O=P(NMe$_2$)$_2$Ind}$_2$]. The halide derivatives were separated as powders, while [Zn(NCS)$_2${O=P(NMe$_2$)$_2$Ind}$_2$] was isolated as oil. The ^{1}H NMR spectra show in all the cases a single set of resonances attributable to the coordinated [O=P]-donor ligands, composed by six multiplets in the aromatic region and a doublet around 2.7–2.8 ppm with $^3J_{PH}$ coupling constant between 10.3 and 10.7 Hz. The ^{1}H NMR chemical shifts in CDCl$_3$ at 298 K display small but definite variations on changing the nature of X and in the case of [Zn(NCS)$_2${O=P(NMe$_2$)$_2$Ind}$_2$] the signals are meaningfully broader, as observable on comparing Figures S1–S4. The ^{31}P{^{1}H} NMR spectra are composed by a singlet in the 17.2–16.3 ppm range, broadened in the case of the thiocyanato complex (Figures S5–S8). The IR spectra show bands related to the vibrations of the [O=P]-donors. The small shifts in the $v_{P=O}$ and v_{P-N} regions with respect to the free ligand are in line with previous reports on related [MnX$_2${O=P(NMe$_2$)$_2$Ind}$_2$] complexes[11r] and are attribut-
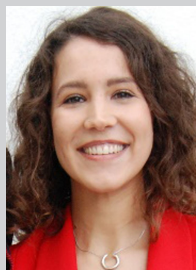
Valentina Ferraro received her B.Sc. and M.Sc. degree in Chemistry and Sustainable Technologies from Ca′ Foscari University of Venice (Italy). She began her Ph.D. in Chemistry under the supervision of Prof. Bortoluzzi in 2019 in a jointed programme between University of Trieste and Ca′ Foscari University of Venice. Her research is currently focused on the synthesis and characterization of luminescent earth-abundant metal complexes, in particular manganese(II), copper(I) and zinc(II) derivatives.
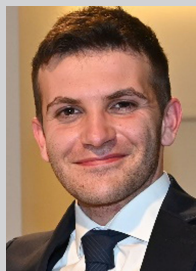
Filippo Baggio received his M.Sc. degree in Chemistry and Sustainable Technologies in 2022 from Ca′ Foscari University of Venice (Italy). His research topic during the internship was the preparation of new luminescent complexes of first row transition metal centres with d[10] configuration.

Prof. Jesús Castro received the M.Sc. degree at the University of Santiago de Compostela (Galicia, Spain) and the Ph.D. in 1993 at the same University under the supervision of Profs. Sousa, García–Vázquez and Romero. After a brief stay at the University of Windsor (Canada) in the group of Prof. Tuck, in 1994 he won an Associate Professor position at the University of Vigo (Galicia, Spain), where he is currently Full Professor. His research focused on coordination compounds with Schiff bases, until in 2004 he began a fruitful collaboration with Profs. Albertin and Antoniutti from Ca′ Foscari University of Venice in the field of organometallic compounds. Nowadays, he collaborates with Prof. Bortoluzzi's group in the synthesis and characterization of luminescent coordination compounds.

Prof. Marco Bortoluzzi received the M.Sc. degree in Industrial Chemistry in 2001 from Ca′ Foscari University of Venice (Italy). He obtained the Ph.D. in Chemical Sciences in 2004. He won the position for permanent researcher at Ca′ Foscari University of Venice in 2007 and from 2020 he is Associate Professor in General and Inorganic Chemistry. His current research activity is centred on the synthesis and characterization of coordination and organometallic compounds of d- and f-block elements. In particular, the study is focused on luminescent complexes to be exploited for optoelectronic applications. The experimental activity is supported by computational calculations, extended to the activation mechanisms of organic molecules by metal complexes and to the electronic structure of metal clusters.

able to the weakening of the O=P bond caused by coordination, with consequent slight enforcement of the P–N bonds.[18] Two strong bands between 2050 and 2100 cm^{-1} are observable in the IR spectrum of [Zn(NCS)$_2${O=P(NMe$_2$)$_2$Ind}$_2$], related to the symmetric and asymmetric stretchings of the coordinated thiocyanato ligands[19] (Figure S9).

Crystals of the halide complexes suitable for X-ray diffraction were collected from dichloromethane/diethyl ether solutions. Crystal data and structure refinement are collected in Table S1. [ZnCl$_2${O=P(NMe$_2$)$_2$Ind}$_2$] and [ZnBr$_2${O=P(NMe$_2$)$_2$Ind}$_2$] are isomorphs and crystallize in the monoclinic $P2_1/n$ space group. [ZnI$_2${O=P(NMe$_2$)$_2$Ind}$_2$] instead crystallizes in the triclinic P-1 space group with two molecules not symmetry related in the asymmetric unity, since one of the NMe$_2$ groups and the indolyl fragment are interchanged around one of the phosphorus atoms (Figure S10). One of the [ZnI$_2${O=P-(NMe$_2$)$_2$Ind}$_2$] molecules is however superimposable with the other halide complexes, as observable in Figure S11. Figure 1 shows the structure of [ZnBr$_2${O=P(NMe$_2$)$_2$Ind}$_2$] as representative example of the three compounds. It is worth noting that the overlay similarity is between 0.96 (Br *vs.* I) and 0.97 (Cl *vs.* Br).[20] High degree of similarity (0.99) was previously found between the related Mn(II) bromo- and iodo-complexes, while the degree of similarity was lower (0.90) on comparing the chloro- and bromo-derivatives.[11r]

In the crystal structure of the three [ZnX$_2${O=P(NMe$_2$)$_2$Ind}$_2$] complexes the metal centre is four-coordinated to two halides and two oxygen atoms in a distorted tetrahedral geometry. In Table S2 the most significant distances and angles are set out, carefully ordered to show the small differences among them. The Zn–X bond lengths are in agreement with the change of the halogen, following the expected sequence Zn–Cl < Zn–Br < Zn–I. The average Zn–O distances become shorter on increasing the Zn–X bond length. Other geometrical parameters in the diamide ligands are not influenced by the nature of the halogen. The P–N(indolyl) bond lengths are always slightly longer than the P-NMe$_2$ ones. The small distortion of the coordination tetrahedron around the zinc atom can be described by the τ_4 parameter,[21] respectively equal to 0.93,
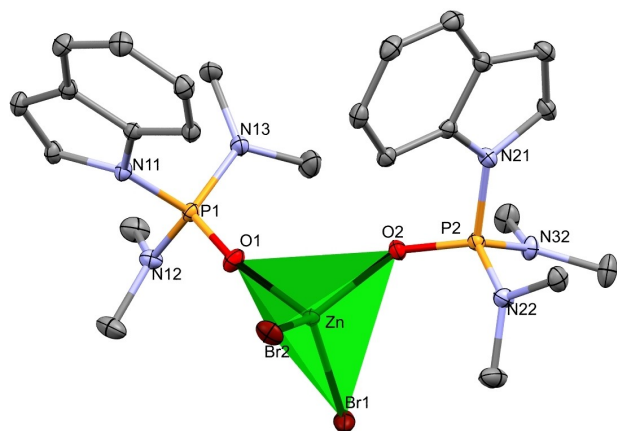
0.92, 0.91 and 0.92 for the chloro- and bromo-complexes and the two molecules of the iodo-species. The values indicate lower distortion from perfect tetrahedron with respect to the related manganese(II) compounds.[11r]

To the best of our knowledge,[22] the long-known phosphine oxide Zn(II) halide compounds[23] were scarcely described from a crystallographic point of view [CSD version 5.41 (update March 2020)]. The crystal structures of halide complexes with triphenylphosphine oxide were reported in few papers, one containing exclusively the bromo-derivative.[12a–c] The structure of the iodo-complex was serendipitously obtained more recently.[24] A THF-solvate of the chloro-compound was also described.[25] On the other hand, polymeric chloro- and iodo-compounds with dppe dioxide were also reported.[26] The diiodo-{pyridine-2,6-diyl-bis[di-*tert*-butyl(phosphinate)]}zinc(II) derivative completes the di-iodo complexes crystallographically deposited at CSD.[27]

The biggest angles around the metal centre in the [ZnX$_2${O=P(NMe$_2$)$_2$Ind}$_2$] complexes are the X–Zn–X ones, while the O–Zn–O are the acutest. The X–Zn–X angle increases on descending along Group 17, from 116.7(1) for [ZnCl$_2${O=P-(NMe$_2$)$_2$Ind}$_2$] to 120.0(1) for [ZnBr$_2${O=P(NMe$_2$)$_2$Ind}$_2$] and to 120.9(1) and 121.2(1) for [ZnI$_2${O=P(NMe$_2$)$_2$Ind}$_2$]. The sequence is exactly in the reverse order for the triad [ZnX$_2$(O=PPh$_3$)$_2$].[12a–c,24] Surprisingly, the O–Zn–O angle does not follow a correlated trend, differently from the triad [ZnX$_2$(O=PPh$_3$)$_2$], and the O–Zn–O angle of [ZnBr$_2${O=P-(NMe$_2$)$_2$Ind}$_2$] is the biggest.

As concerns the disposition of the indolyl substituents, the dihedral angle between the planes of the two heterocycles in the same molecule increases along Group 17, being 57.39(4), 63.14(4) and 74.01(7)° respectively for X = Cl, Br and I. In the second configuration of [ZnI$_2${O=P(NMe$_2$)$_2$Ind}$_2$] the dihedral angle is 61.5(1)°. The P–N bond vectors generate angles with the indolyl plane equal to 12.27(5) and 8.97(5)° for [ZnCl$_2${O=P-(NMe$_2$)$_2$Ind}$_2$], 12.98(5) and 7.20(5)° for the [ZnBr$_2${O=P-(NMe$_2$)$_2$Ind}$_2$] and 10.56(8) and 4.11(8)° for [ZnI$_2${O=P-(NMe$_2$)$_2$Ind}$_2$]. The values for the other molecule in the asymmetric unit of the iodo-derivative are 10.24(8) and 13.67(9)°. The lack of similarity between the three complexes probably relies on the P–O–Zn angles. The range observed for triphenylphosphine oxide Zn(II) halide complexes is comprised between 145 and 155°, with the exception of the THF-solvated [ZnCl$_2$(O=PPh$_3$)$_2$], where the values are 139.20(9) and 141.01(9)°.[12a–c,25] On the contrary, in the complexes here reported only one of the ligands exhibits a O–P–Zn angle roughly comparable to the triphenylphosphine oxide derivatives, but the other one is considerably different. For instance, in [ZnCl$_2${O=P(NMe$_2$)$_2$Ind}$_2$] one angle is equal to 140.40(6)°, slightly acuter than the previously mentioned range, but the other one is even acuter and equal to 134.14(5)°. In [ZnBr$_2${O=P-(NMe$_2$)$_2$Ind}$_2$] one of the angles is equal to 145.23(6)°, but the other one is more linear and equal to 165.75(7)°. Similar behaviour was found in one of the molecules of [ZnI$_2${O=P-(NMe$_2$)$_2$Ind}$_2$], where one of the angles is equal to 146.30(10)°, but the other one considerably deviates and it is equal to 163.92(10)°. Nevertheless, the other molecule found in the

Figure 1. X-ray structure of [ZnBr$_2${O=P(NMe$_2$)$_2$Ind}$_2$].

asymmetric unit of [ZnI₂{O=P(NMe₂)₂Ind}₂], that is different from the other halide complexes, has Zn–O–P angles equal to 143.94(10) and 152.55(10)°, falling in the triphenylphosphine oxide range.

Despite the fact that [Zn(NCS)₂{O=P(NMe₂)₂Ind}₂] was isolated as an oil, the formation of a four-coordinated complex is supported by the characterization data and the possible structure was simulated by means of DFT calculations. The coordination through the nitrogen atom of the two thiocyanate ions is favoured with respect to the interaction through sulphur by about 24.9 kcal mol^{-1}. The most stable isomer has slightly distorted tetrahedral geometry, as observable in Figure S12 (computed τ_4 value equal to 0.91). Selected computed bond lengths and angles are provided in the caption of Figure S12. The simulated IR spectrum is in accordance with the experimental one, being the computed unscaled values for the ν_{CN} stretching vibrations equal to 2173 (symmetric) and 2153 (asymmetric) cm^{-1}.

Photoluminescence of [ZnX₂{O=P(NMe₂)₂Ind}₂ (X=Br, I)

[ZnBr₂{O=P(NMe₂)₂Ind}₂] and [ZnI₂{O=P(NMe₂)₂Ind}₂] exhibited bright green emissions upon excitation with UV light below 300 nm at the solid state. On the other hand, the photoluminescence of the related chloro-compound and thiocyanato-complex was negligible, and for this reason the attention was focused on the complexes with the heavier halides in the coordination sphere. On considering the emission features described below for the bromo- and iodo-derivatives, the lack of luminescence of [ZnCl₂{O=P(NMe₂)₂Ind}₂] and [Zn(NCS)₂{O=P-(NMe₂)₂Ind}₂] appears attributable to the absence of atoms in the Zn(II) first coordination sphere able to induce strong intersystem crossing. No appreciable luminescence was observed for the compounds in solution, probably because of vibrational coupling with solvent molecules. All the measurements were therefore carried out on crystallized solid samples. No changes on the emission properties were detected upon grinding.

Emission (PL) and excitation (PLE) spectra are reported in Figure 2. The spectra are identical under inert atmosphere and under air. The PL spectrum of [ZnBr₂{O=P(NMe₂)₂Ind}₂] is composed by a single band centred at 531 nm, with full-width half-maximum (FWHM) around 2900 cm^{-1}. Despite the comparable emission range, the PL spectrum of [ZnI₂{O=P(NMe₂)₂Ind}₂] is different, being composed by a set of shoulders and peaks, the most intense falling at 521 nm. The peaks are all separated by about 1300 cm^{-1} (see the interpolation provided in Figure S13), suggesting that the ground-state vibrational structure is subtended by the PL spectrum. The quite high wavenumber is most likely related to vibrations in the O=P(NMe₂)₂Ind ligands, since much lower values are expected for vibrations involving the Zn(II) first coordination sphere.[28] Despite the fact that solid samples allow only qualitative comparisons, Figure 2 clearly highlights that [ZnBr₂{O=P(NMe₂)₂Ind}₂] is much more luminescent than the related iodo-complex under the same experimental conditions.

The PL spectra do not vary on changing the excitation wavelength and the two compounds have roughly superimposable PLE spectra. The excitation range at the solid state is limited to wavelengths shorter than 330 nm and it is comparable to the absorption interval obtained for dichloromethane
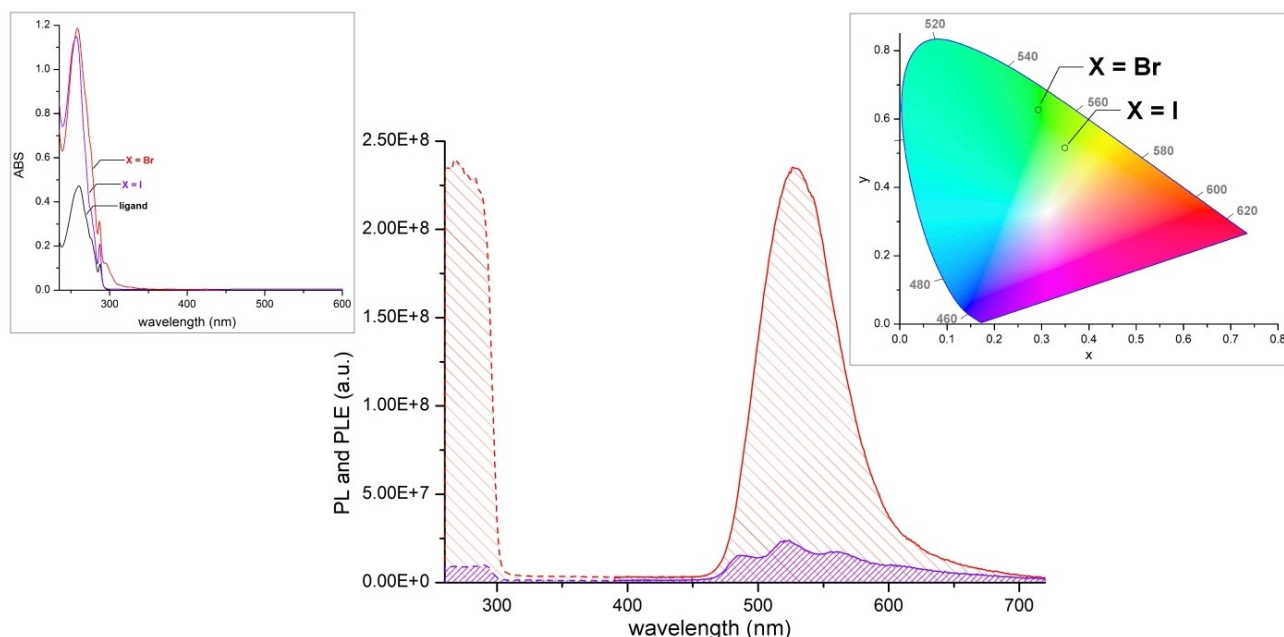

Figure 2. PL (solid lines) and PLE (dashed lines) spectra of [ZnBr₂{O=P(NMe₂)₂Ind}₂] (red lines) and [ZnI₂{O=P(NMe₂)₂Ind}₂] (violet lines). Solid samples, r.t., $\lambda_{\text{excitation}}=290$ nm, $\lambda_{\text{emission}}=520$ nm, intensities in arbitrary units. Inset: absorption spectra of a $5\cdot10^{-5}$ M solution in CH₂Cl₂ of [ZnX₂{O=P(NMe₂)₂Ind}₂] (X=Br, I) and of the free ligand. Inset: CIE 1931 chromaticity diagram.

Table 1. Selected photoluminescence and electrochemistry data for [ZnX$_2${O=P(NMe$_2$)$_2$Ind}$_2$] (X = Br, I)

	PL max[a,b] (nm)	PLE[a,c] (nm)	CIE coordinates	τ[a–d] (ms)	τ[a–c,e] (ms)	Φ[a,d,f] (%)	Ox onset[d,g] (V vs Fc$^+$/Fc)	Red onset[d,g] (V vs Fc$^+$/Fc)
[ZnBr$_2${O=P(NMe$_2$)$_2$Ind}$_2$]	531	<310	x = 0.293, y = 0.627	0.70	0.40	19	0.95	−1.41
[ZnI$_2${O=P(NMe$_2$)$_2$Ind}$_2$]	521	<330	x = 0.349, y = 0.516	2.58	2.60	7	0.30, 0.97	−1.51

[a] Solid sample, r.t. [b] $\lambda_{excitation}$ = 290 nm. [c] $\lambda_{emission}$ = 520 nm. [d] Under inert atmosphere. [e] Under air. [f] $\lambda_{excitation}$ = 310 nm. [g] CH$_3$CN/LiClO$_4$, r.t. glassy carbon electrode, ferrocene as internal standard, scan rate 100 mV/s.

solutions of the complexes (Figure 2). The absorption spectrum of the complexes is strictly comparable to that of the free ligand, therefore the excitation causing the emission is mainly ascribed to $\pi^* \leftarrow \pi$ absorptions of the coordinated ligands. No absorption in the visible range was detected also for concentrated solutions of the complexes (see for instance in Figure S14).

As observable in Figure 2, the emissions of both [ZnBr$_2${O=P(NMe$_2$)$_2$Ind}$_2$] and [ZnI$_2${O=P(NMe$_2$)$_2$Ind}$_2$] fall in the yellowish green region of the CIE 1931 diagram, with colour purity values around 0.78 and 0.61 for the bromo- and the iodo-complex, respectively. The photoluminescence quantum yields (Φ) at room temperature are 19% for [ZnBr$_2${O=P(NMe$_2$)$_2$Ind}$_2$] and 7% for [ZnI$_2${O=P(NMe$_2$)$_2$Ind}$_2$]. The lower value obtained for the iodo-derivative is perhaps related to expansion of the emission band towards higher wavelengths, favouring non-radiative decay routes. Photoluminescence data are summarized in Table 1 for clarity.

The large Stokes shifts observable in Figure 2 are quite uncommon for zinc(II) luminescent complexes. The lifetimes of the excited states obtained from the monoexponential fit of the luminescence decay curves provided in Figure 3 are in the milliseconds range, respectively 0.70 ms for [ZnBr$_2${O=P(NMe$_2$)$_2$Ind}$_2$] and 2.58 ms for [ZnI$_2${O=P(NMe$_2$)$_2$Ind}$_2$], strongly supporting the idea that triplet excited states are involved in the emissions. Such a hypothesis is in line with the absence of comparable photoluminescence from the related chloro- and thiocyanato-complexes. This outcome can be justified consider-
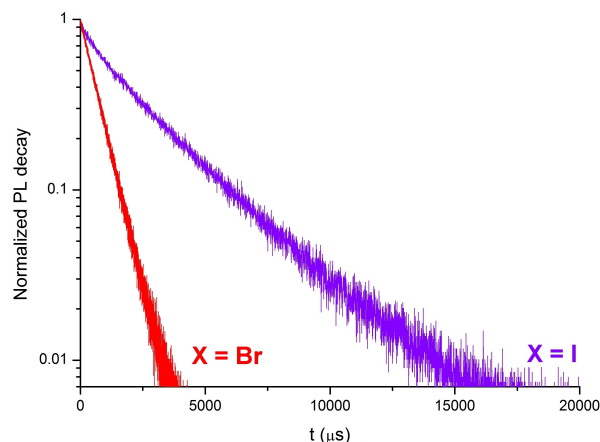

Figure 3. Semi-log plots of the luminescence decay curves of [ZnBr$_2${O=P-(NMe$_2$)$_2$Ind}$_2$] (red line) and [ZnI$_2${O=P(NMe$_2$)$_2$Ind}$_2$] (violet line). Solid samples, r.t., $\lambda_{excitation}$ = 290 nm, $\lambda_{emission}$ = 520 nm.

ing the lack of heavy atoms directly coordinated to the metal centre which can favour the intersystem crossing. The linear semi-log plots of the luminescence decays indicate the presence of a single emitting level. The lifetimes here provided are in the same time scale of those recently reported for coordination polymers based on [Zn$_3$(HPO$_3$)$_2$]$^{2+}$ cations linked by 1,3,5-tris(1-imidazolyl)-benzene.[9b]

To shed light on the photoluminescence of the N,N,N',N'-tetramethyl-P-indol-1-ylphosphonic diamide complexes, measurements were carried out under the same experimental conditions on the analogous triphenylphosphine oxide derivatives. [ZnI$_2$(O=PPh$_3$)$_2$] showed no appreciable photoluminescence and it was not further investigated. On the other hand, the emission spectrum of [ZnBr$_2$(O=PPh$_3$)$_2$] is dominated by a peak at 403 nm, with shoulders at about 440 and 504 nm (Figure S15). The lifetime is around 5 ns (Figure S15). The completely different behaviour of the triphenylphosphine oxide complexes clearly highlights the role of the indolyl-substituted phosphoramide in the luminescence of the corresponding ZnBr$_2$ and ZnI$_2$ complexes.

Electrochemical measurements showed that O=P(NMe$_2$)$_2$Ind is more reducing than O=PPh$_3$. Both the ligands give irreversible oxidation processes, but the onset of the oxidation of O=P-(NMe$_2$)$_2$Ind falls at potential about 200 mV lower than that of O=PPh$_3$. The oxidation of O=P(NMe$_2$)$_2$Ind occurs at lower potential with respect to ZnBr$_2$ and it is more or less coincident with the second oxidation peak of ZnI$_2$ (Figure S16). The cyclic voltammograms of [ZnBr$_2${O=P(NMe$_2$)$_2$Ind}$_2$] and [ZnI$_2${O=P-(NMe$_2$)$_2$Ind}$_2$], compared to those of the corresponding zinc halides, are shown in Figure 4. The oxidation process of the bromo-derivative starts around 0.95 V, roughly at the same potential of the free ligand. An analogous process is observable for the iodo-complex, anticipated by an irreversible oxidation centred at about 0.43 V related to coordinated iodide. The reduction processes occur at potential lower than -1.4 V for [ZnBr$_2${O=P(NMe$_2$)$_2$Ind}$_2$] and -1.5 V for [ZnI$_2${O=P(NMe$_2$)$_2$Ind}$_2$], and are comparable to those observed for the related ZnX$_2$ halides, with little shifts at lower potentials. The onsets of the ligand-centred oxidation and metal-centred reduction processes are separated by about 2.45–2.50 V, corresponding to an energy difference in the same range of the emissions of the complexes. Selected data are summarized in Table 1.

Despite the results obtained from cyclic voltammetry, the lack of LMCT bands in the absorption spectra (Figures 2 and S14) does not agree with emissions attributable to charge-transfer transitions.
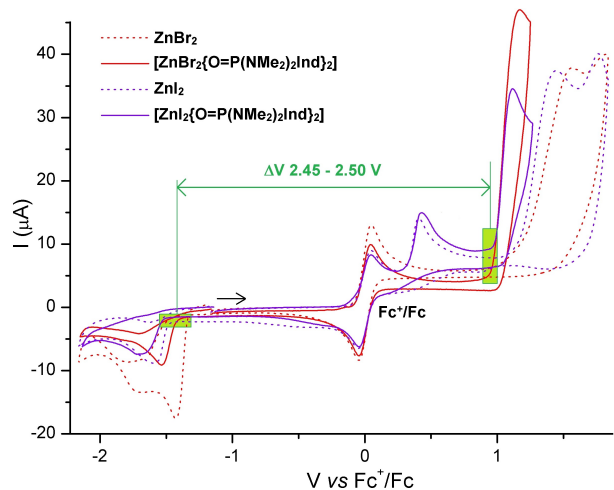
Figure 4. Cyclic voltammograms of [ZnBr$_2${O=P(NMe$_2$)$_2$Ind}$_2$] (solid red line), [ZnI$_2${O=P(NMe$_2$)$_2$Ind}$_2$] (solid violet line), ZnBr$_2$ (dotted red line) and ZnI$_2$ (dotted violet line). CH$_3$CN/LiClO$_4$, r.t., glassy carbon electrode, ferrocene (Fc) as internal reference, scan rate 100 mV/s.

Lifetime measurements carried out on the solid samples under air instead of inert atmosphere revealed a meaningful reduction of the τ value for [ZnBr$_2${O=P(NMe$_2$)$_2$Ind}$_2$], from 0.70 to 0.40 ms (Figure S17 and Table 1). On the other hand, the lifetime of [ZnI$_2${O=P(NMe$_2$)$_2$Ind}$_2$] resulted negligibly affected by the presence of air. This outcome, together with the different profiles of the PL spectra of the two compounds, may suggest different luminescence mechanisms, but the large Stokes shifts and the long lifetimes strongly indicate in both the cases the participation of excited triplet states.

The possible nature of the PL bands was also investigated by means of DFT and TD-DFT calculations. The DFT-optimized geometries of the two complexes in triplet configuration are strictly similar to the related singlet ground states (see Figure S18), without meaningful variations in the first coordination spheres. The zinc centre appears therefore poorly affected by the change of multiplicity of the molecules. The computed energy values for the T$_1$→S$_0$ transitions at the triplet equilibrium geometries are 2.06 eV for [ZnBr$_2${O=P(NMe$_2$)$_2$Ind}$_2$] and 2.36 eV for [ZnI$_2${O=P(NMe$_2$)$_2$Ind}$_2$], in acceptable agreement with the experimental data. The hole and electron distributions[29] associated to the emission transition, plotted in Figure 5, confirm that the electron moves between π-delocalized orbitals of the same indolyl fragment, with negligible contribution of the remaining parts of the molecules. On the basis of the TD-DFT outcomes the transitions are therefore ascribed to ligand-centred processes, not detected for the free *N,N,N',N'*-tetramethyl-*P*-indol-1-ylphosphonic diamide.[11r] The role attributable to the zinc(II) heavy halide fragments is the enhancement of the intersystem crossing between excited singlet and triplet states of the coordinated ligands.
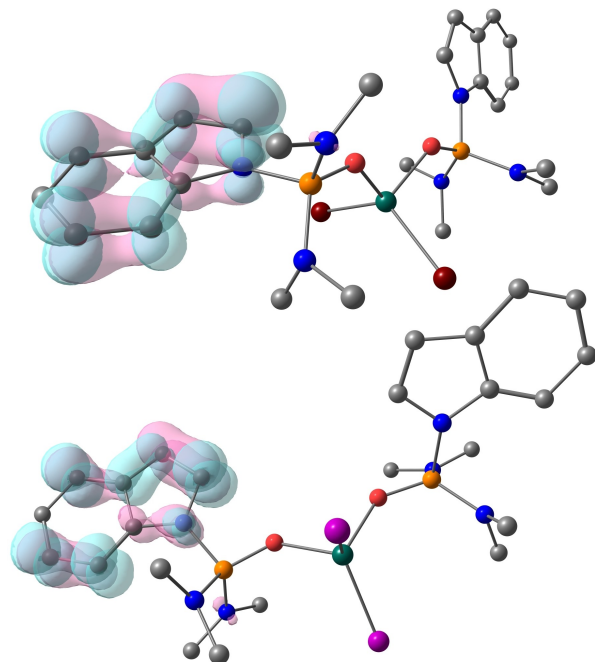

Figure 5. DFT-optimized triplet state geometries of [ZnBr$_2${O=P(NMe$_2$)$_2$Ind}$_2$] and [ZnI$_2${O=P(NMe$_2$)$_2$Ind}$_2$] with hole (light blue) and electron (light pink) distributions related to the T$_1$→S$_0$ transitions (surface isovalue = 0.003 a.u.). Colour map: C, grey; N, blue; O, red; P, orange; Zn, dark green; Br, dark red; I, violet. Hydrogen atoms are omitted for clarity.

Conclusion

The investigation on neutral tetrahedral zinc(II) complexes with functionalized phosphoramides revealed the possibility to obtain compounds with quite simple molecular design characterized by bright emission in the visible range. The photoluminescence of [ZnBr$_2${O=P(NMe$_2$)$_2$Ind}$_2$] and [ZnI$_2${O=P-(NMe$_2$)$_2$Ind}$_2$] is characterized by large Stokes shifts and long lifetimes, accordingly to emission from excited triplet states. Such a situation is relatively uncommon for zinc(II) complexes, usually characterized by fluorescent emissions, and it is related the presence of heavy atoms in the first coordination sphere. The emissions of the new compounds are attributable to ligand-centred transitions involving triplet states on the basis of experimental observations and theoretical calculations, with central role of the indolyl substituents. The excitation of the complexes is due to singlet←singlet transitions centered on the π-system of the coordinated phosphoramides.

The earth abundance and negligible toxicity of zinc makes this element a promising candidate for the development of new luminescent compounds to be applied in advanced technology. Further studies will be carried out to verify if ZnX$_2$ centres with heavy halides are able to promote the intersystem crossing in further [O=P]-donor ligands with suitable π-delocalized fragments, in order to verify the flexibility and the limits of this approach for the synthesis of inexpensive photoluminescent compounds.

Experimental Section

General Remarks

Commercial solvents (Aldrich) were purified as described in the literature.[30] Anhydrous Zn(II) halides were purchased from Merck, as well as all the organic reactants. $Zn(NCS)_2$ was prepared from the reaction between $ZnSO_4 \cdot 7H_2O$ and K[NCS] in methanol.[31] All the syntheses were carried out under inert atmosphere, working in a glove box (MBraun Labstar with MB 10 G gas purifier) filled with N_2 and equipped for organic and inorganic syntheses. N,N,N',N'-tetramethyl-P-indol-1-ylphosphonic diamide $O=P(NMe_2)_2Ind$ was synthesized on the basis of the methods reported in the literature.[32] Elemental analyses (C, H, N) were carried out using an Elementar Unicube microanalyzer. Halide content was determined using the Mohr's method.[33] Melting points were registered employing a FALC 360 D instrument equipped with a camera. Cyclic voltammetry measurements were performed using an eDAQ ET014-199 instrument in acetonitrile containing 0.1 M $LiClO_4$. All the measurements were carried out under argon at room temperature. The working electrode was 1-mm glassy carbon disk, while the auxiliary electrode was Pt-coated titanium rod. The electrodes were provided by eDAQ. Ferrocene was introduced as internal standard and a Pt wire was used as pseudo-reference electrode. IR spectra were collected in the 4000–400 cm^{-1} range using a Perkin-Elmer Spectrum One spectrophotometer. Mono- and bidimensional nuclear magnetic resonance (NMR) spectra were collected employing Bruker Avance 300 and Avance 400 instruments operating respectively at 300.13 MHz and 400.13 MHz of protonic resonance. ^1H NMR spectra are referred to the partially non-deuterated fraction of the solvent, itself referred to tetramethyl silane. $^{31}P\{^1H\}$ NMR resonances are referred to 85% H_3PO_4 in water. Absorption spectra in dichloromethane were collected in the 235–700 nm range employing a Perkin-Elmer Lambda 40 spectrophotometer. Photoluminescence emission (PL) and excitation (PLE) spectra as well as lifetime decay curves were registered on solid samples at room temperature using a Horiba Jobin Yvon Fluorolog-3 spectrofluorometer. Air-tight quartz sample holders were used and filled in the glove box to avoid interactions of the air-sensible complexes with moisture. A continuous wave xenon arc lamp was used as source and the excitation wavelength was selected using a double Czerny-Turner monochromator. Suitable long pass filters were placed in front of the acquisition systems. The detector was composed of a single monochromator iHR320 and a photomultiplier tube Hamamatsu R928. Excitation and emission spectra were corrected for the instrumental functions. Time-resolved analyses were performed in Multi Channel Scaling modality (MCS) by using a pulsed UV LED source centred at 290 nm or in TCSPC (time correlated single photon counting) mode employing a Horiba NanoLED centred at 373 nm. The photoluminescence quantum yields (Φ) in the solid state at room temperature was measured by means of an Ocean-Optics HR4000CG UV-NIR detector, fiber-coupled to an integrating sphere connected to an OceanOptics LED source centred at 310 nm. Values are reported as average of three measurements.

Synthesis of the [ZnX$_2${O=P(NMe$_2$)$_2$Ind}$_2$] Complexes (X=Cl, Br, I, NCS)

The complexes were prepared by slowly adding a solution containing 2.1 mmol of N,N,N',N'-tetramethyl-P-indol-1-ylphosphonic diamide into a solution of the proper zinc(II) precursor (1 mmol: 0.136 g for $ZnCl_2$, 0.225 g for $ZnBr_2$, 0.319 g for ZnI_2, 0.182 g for $Zn(NCS)_2$) dissolved in 20 mL of EtOH. The reaction mixture was stirred overnight inside the glove box at room temperature. The solvent was then evaporated under reduced pressure and the product was isolated by adding diethyl ether. The

solid was then filtered and dried *in vacuo*. Only in the case of [Zn(NCS)$_2${O=P(NMe$_2$)$_2$Ind}$_2$] the product was kept as an oil. Crystal of the [ZnX$_2${O=P(NMe$_2$)$_2$Ind}$_2$] (X=Cl, Br, I) suitable for X-ray diffraction were collected from dichloromethane/diethyl ether solutions. Yields: 0.460 g (72%) for X=Cl, 0.546 g (75%) for X=Br, 0.583 g (71%) for X=I, 0.212 g (31%) for X=NCS.

Characterization of [ZnCl$_2${O=P(NMe$_2$)$_2$Ind}$_2$]. Anal. calcd for $C_{24}H_{36}Cl_2N_6O_2P_2Zn$ (638.83 g mol^{-1}, %): C, 45.12; H, 5.68; N, 13.16; Cl, 11.10. Found (%): C, 44.94; H, 5.70; N, 13.11; Cl, 11.07. M.p. 125 °C (dec.). ^1H NMR (CDCl$_3$, 298 K) δ 7.84 (d, 2H, $^3J_{HH}=8.1$ Hz, Ind), 7.60 (d, 2H, $^3J_{HH}=7.7$ Hz, Ind), 7.25 (m, 2H, Ind), 7.19 (t, 2H, $^3J_{HH}=7.5$ Hz, Ind), 7.14 (t, 2H, $^3J_{HH}=7.5$ Hz, Ind), 6.64 (m, 2H, Ind), 2.77 (d, 24H, $^3J_{PH}=10.5$ Hz, N–Me). $^{31}P\{^1H\}$ NMR (CDCl$_3$, 298 K) δ 17.20 (FWHM = 7 Hz). IR (KBr, cm^{-1}): 3140–3005 m (aromatic ν$_{C-H}$), 2990–2820 m (ν$_{C-H}$), 1530–1450 m (aromatic ν$_{C-C}$ and ν$_{C-N}$), 1180–1120 s (ν$_{P=O}$ and ν$_{C-N}$), 1010–1000 s (ν$_{P-N}$). UV-VIS (CH$_2$Cl$_2$, 298 K, nm) <300, 257 (max), 274 (sh), 287 (sh).

Characterization of [ZnBr$_2${O=P(NMe$_2$)$_2$Ind}$_2$]. Anal. calcd for $C_{24}H_{36}Br_2N_6O_2P_2Zn$ (727.73 g mol^{-1}, %): C, 39.61; H, 4.99; N, 11.55; Br, 21.96. Found (%): C, 39.45; H, 5.01; N, 11.50; Br, 22.05. M.p. 205 °C (dec.). ^1H NMR (CDCl$_3$, 298 K) δ 7.86 (d, 2H, $^3J_{HH}=8.0$ Hz, Ind), 7.60 (d, 2H, $^3J_{HH}=7.7$ Hz, Ind), 7.25 (m, 2H, Ind), 7.19 (t, 2H, $^3J_{HH}=7.3$ Hz, Ind), 7.13 (t, 2H, $^3J_{HH}=7.6$ Hz, Ind), 6.64 (m, 2H, Ind), 2.78 (d, 24H, $^3J_{PH}=10.6$ Hz, N–Me). $^{31}P\{^1H\}$ NMR (CDCl$_3$, 298 K) δ 17.11 (FWHM = 7 Hz). IR (KBr, cm^{-1}): 3130–3005 m (aromatic ν$_{C-H}$), 2950–2820 m (ν$_{C-H}$), 1525–1450 m (aromatic ν$_{C-C}$ and ν$_{C-N}$), 1210–1120 s (ν$_{P=O}$ and ν$_{C-N}$), 1010–950 s (ν$_{P-N}$). UV-VIS (CH$_2$Cl$_2$, 298 K, nm) <300, 260 (max), 276 (sh), 287 (sh). PL (solid, r.t., λ$_{excitation}=290$ nm, nm): 531 (FWHM = 2900 cm^{-1}). CIE 1931 coordinates: x=0.293, y=0.627. PLE (solid, r.t., λ$_{emission}=520$ nm, nm) <310. τ (solid, r.t., λ$_{excitation}=$ 290 nm, λ$_{emission}=520$ nm, ms): 0.70. Φ (solid, r.t., λ$_{excitation}=310$ nm): 19%.

Characterization of [ZnI$_2${O=P(NMe$_2$)$_2$Ind}$_2$]. Anal. calcd for $C_{24}H_{36}I_2N_6O_2P_2Zn$ (821.73 g mol^{-1}, %): C, 35.08; H, 4.42; N, 10.23; I, 30.89. Found (%): C, 34.94; H, 4.46; N, 10.19; I, 30.77. M.p. 122 °C (dec.). ^1H NMR (CDCl$_3$, 298 K) δ 7.89 (d, 2H, $^3J_{HH}=8.2$ Hz, Ind), 7.59 (d, 2H, $^3J_{HH}=7.8$ Hz, Ind), 7.23 (m, 2H, Ind), 7.19 (t, 2H, $^3J_{HH}=7.3$ Hz, Ind), 7.13 (t, 2H, $^3J_{HH}=7.9$ Hz, Ind), 6.64 (m, 2H, Ind), 2.78 (d, 24H, $^3J_{PH}=10.7$ Hz, N–Me). $^{31}P\{^1H\}$ NMR (CDCl$_3$, 298 K) δ 16.36 (FWHM = 7 Hz). IR (KBr, cm^{-1}): 3130–3005 m/w (aromatic ν$_{C-H}$), 2950–2820 m (ν$_{C-H}$), 1525–1450 m (aromatic ν$_{C-C}$ and ν$_{C-N}$), 1210–1120 s (ν$_{P=O}$ and ν$_{C-N}$), 1010–950 s (ν$_{P-N}$). UV-VIS (CH$_2$Cl$_2$, 298 K, nm) <300, 257 (max), 275 (sh), 287 (sh). PL (solid, r.t., λ$_{excitation}=290$ nm, nm): 487 (sh), 521 (max), 559, 604 (sh), 655 (sh). CIE 1931 coordinates: x=0.349, y=0.516. PLE (solid, r.t., λ$_{emission}=520$ nm, nm) <330. τ (solid, r.t., λ$_{excitation}=290$ nm, λ$_{emission}=520$ nm, ms): 2.58. Φ (solid, r.t., λ$_{excitation}=310$ nm): 7%.

Characterization of [Zn(NCS)$_2${O=P(NMe$_2$)$_2$Ind}$_2$]. Anal. calcd for $C_{26}H_{36}N_8O_2P_2S_2Zn$ (684.08 g mol^{-1}, %): C, 45.65; H, 5.30; N, 16.38. Found (%): C, 45.47; H, 5.33; N, 16.45. ^1H NMR (CDCl$_3$, 298 K) δ 7.69 (m, br, 2H, Ind), 7.59 (m, 2H, Ind), 7.19 (m, br, 4H, Ind), 7.11 (m, br, 2H, Ind), 6.67 (m, br, 2H, Ind), 2.69 (d, br, 12H, $^3J_{PH}=10.3$ Hz, N–Me). $^{31}P\{^1H\}$ NMR (CDCl$_3$, 298 K) δ 17.22 (FWHM = 32 Hz). IR (cm^{-1}): 2087, 2064 vs (ν$_{CN}$), 1527 s, 1481 s, 1472 s, 1449 s (ν$_{arom}$), 1160 s (ν$_{P=O}$).

Crystal Structure Determination

Crystallographic data were collected at CACTI (Univ. of Vigo) at 100 K (CryoStream 800) using a Bruker D8 Venture Photon II CMOS detector and Mo–Kα radiation (λ=0.71073 Å) generated by a Incoatec Microfocus Source IμS. The software APEX3[34] was used for collecting frames of data, indexing reflections, and the determination of lattice parameters, SAINT[34] for integration of intensity of reflections, and SADABS[34] for scaling and empirical absorption

correction. The crystallographic treatment was performed with the Oscail program,[35] solved using the SHELXT program.[36] The structure was subsequently refined by a full-matrix least-squares based on F^2 using the SHELXL program.[37] Non-hydrogen atoms were refined with anisotropic displacement parameters. Hydrogen atoms were included in idealized positions and refined with isotropic displacement parameters. Further details concerning crystal data and structural refinement are given in Table 1. CCDC 2094664 for [ZnCl$_2${O=P(NMe$_2$)$_2$Ind}$_2$], 2094665 for [ZnBr$_2${O=P-(NMe$_2$)$_2$Ind}$_2$] and 2094666 for [ZnI$_2${O=P(NMe$_2$)$_2$Ind}$_2$] contain the supplementary crystallographic data for this paper. PLATON (version 290122)[38] was used to obtain some geometrical parameters from the cif files.

Computational Calculations

The ground-state geometry optimizations were carried out using the range-separated hybrid DFT functional TPSSh[39] in combination with Alhrichs' split-valence basis set def2-SVP, with ECP including 28 electrons for iodine.[40] The stationary points were characterized by means of IR simulation (harmonic approximation). Excited states and their relative energies were investigated by means of TD-DFT (time-dependent DFT) calculations at the same theoretical level.[41] The software used was Gaussian 16.[42] The output files were elaborated to obtain the hole and electron distributions with the software MultiWFN, version 3.5.[43] Cartesian coordinates of the DFT-optimized structures are provided in Tables S3–S5.

Acknowledgements

Conflict of Interest

The authors declare no conflict of interest.

Data Availability Statement

The data that support the findings of this study are available in the supplementary material of this article.

[1] a) K. E. Dalle, J. Warnan, J. J. Leung, B. Reuillard, I. S. Karmel, E. Reisner, *Chem. Rev.* **2019**, *119*, 2752–2875; b) M. Freitag, J. Teuscher, Y. Saygili, X. Zhang, F. Giordano, P. Liska, J. Hua, S. M. Zakeeruddin, J.-E. Moser, M. Grätzel, A. Hagfeldt, *Nat. Photonics* **2017**, *11*, 372–378; c) E. Baranoff, in *Organometallics and Related Molecules for Energy Conversion*, (Ed: W. Y. Wong), Springer, Heidelberg, Germany, **2015**, pp. 61–90; d) L. A. Bűldt, O. S. Wenger, *Chem. Sci.* **2017**, *8*, 7359–7367.

[2] a) C. Bizzarri, E. Spuling, D. M. Knoll, D. Volz, S. Bräse, *Coord. Chem. Rev.* **2018**, *373*, 49–82; b) C. Wegeberg, O. Wenger, *JACS Au* **2021**, *1*, 1860–1876; c) O. Wenger, *J. Am. Chem. Soc.* **2018**, *140*, 13522–13533; d) G. Umuhire Mahoro, J. Fernandez-Cestau, J.-L. Renaud, P. B. Coto, R. D. Costa, S. Gaillard, *Adv. Opt. Mater.* **2020**, *8*, 2000260; e) L. A. Büldt, X. Guo, R. Vogel, A. Prescimone, O. S. Wenger, *J. Am. Chem. Soc.* **2017**, *139*, 985–992.

[3] a) R. D. Costa, E. Ortí, H. J. Bolink, F. Monti, G. Accorsi, N. Armaroli, *Angew. Chem. Int. Ed.* **2012**, *51*, 8178–8211; *Angew. Chem.* **2012**, *124*, 8300–8334; b) H. Yersin, A. F. Rausch, R. Czerwieniec, T. Hofbeck, T. Fischer, *Coord. Chem. Rev.* **2011**, *255*, 2622–2652; c) W. C. H. Choy, W. K. Chan, Y. Yuan, *Adv. Mater.* **2014**, *26*, 5368–5399; d) L. Wang, Z. Zhao, C. Wei, H. Wei, Z. Liu, Z. Bian, C. Huang, *Adv. Opt. Mater.* **2019**, *7*, 1801256; e) K.-H. Kim, J.-J. Kim, *Adv. Mater.* **2018**, *30*, 1705600; f) G. B. Bodedla, D. N. Tritton, X. Chen, J. Zhao, Z. Guo, K. C.-F. Leung, W.-Y. Wong, X. Zhu, *ACS Appl. Mater. Interfaces* **2021**, *4*, 3945–3951.

[4] a) L.-J. Xu, C.-Z. Sun, H. Xiao, Y. Wu, Z.-N. Chen, *Adv. Mater.* **2017**, *29*, 1605739; b) Y. Qin, P. She, X. Huang, W. Huang, Q. Zhao, *Coord. Chem. Rev.* **2020**, *416*, 213331; c) P. Tao, S.-J. Liu, W.-Y. Wong, *Adv. Opt. Mater.* **2020**, *8*, 2000985; d) Y. Y. Qin, P. Tao, L. Gao, P. F. She, S. J. Liu, X. L. Li, F. Y. Li, H. Wang, Q. Zhao, Y. Q. Miao, W. Huang, *Adv. Opt. Mater.* **2019**, *7*, 1801160; e) L. P. Ravaro, K. P. S. Zanoni, A. S. S. de Camargo, *Energy Rep.* **2020**, *6*, 37–45; f) L. Liu, S.-C. Yiu, C.-L. Ho, W.-Y. Wong, *Coord. Chem. Rev.* **2018**, *375*, 514–557; g) R. Hamze, J. L. Peltier, D. Sylvinson, M. Jung, J. Cardenas, R. Haiges, M. Soleilhavoup, R. Jazzar, P. I. Djurovich, G. Bertrand, M. E. Thompson, *Science* **2019**, *363*, 601–606.

[5] a) F. Dumur, *Synth. Met.* **2014**, *195*, 241–151; b) G. A. Ardizzoia, S. Brenna, S. Durini, B. Therrien, M. Veronelli, *Eur. J. Inorg. Chem.* **2014**, 4310–4319; c) G. Volpi, E. Priola, C. Garino, A. Daolio, R. Rabezzana, P. Benzi, A. Giordana, E. Diana, R. Gobetto, *Inorg. Chim. Acta* **2020**, *509*, 119662; d) G. A. Ardizzoia, G. Colombo, B. Therrien, S. Brenna, *Eur. J. Inorg. Chem.* **2019**, 1825–1831; e) S. Di Bella, *Dalton Trans.* **2021**, *50*, 6050–6053; f) G. A. Ardizzoia, S. Brenna, S. Durini, B. Therrien, *Polyhedron* **2015**, *90*, 214–220; g) H.-W. Zheng, M. Wu, D.-D. Yang, Q.-F. Liang, J.-B. Li, X.-J. Zheng, *Inorg. Chem.* **2021**, *60*, 11609–11615; h) A. N. Gusev, M. A. Kiskin, E. V. Braga, M. A. Kryukova, G. V. Baryshnikov, N. N. Karaush-Karmazin, V. A. Minaeva, B. F. Minaev, K. Ivaniuk, P. Stakhira, H. Ågren, W. Linert, *ACS Appl. Electron. Mater.* **2021**, *3*, 3436–3444; i) R. Lakshmanan, N. C. Shivaprakash, S. Sindhu, *J. Lumin.* **2018**, *196*, 136–145; j) A. S. Burlov, V. G. Vlasenko, Y. V. Koshchienko, M. S. Milutka, E. I. Mal'tsev, A. V. Dmitriev, D. A. Lypenko, N. V. Nekrasova, A. A. Kolodina, N. I. Makarova, A. V. Metelitsa, V. A. Lazarenko, Y. V. Zubavichus, V. N. Khrustalev, D. A. Garnovskii, *Appl. Organomet. Chem.* **2021**, *35*, e6107; k) A. Ogunsipe, D. Maree, T. Nyokong, *J. Mol. Struct.* **2003**, *650*, 131–140; l) D. Tungulin, J. Leier, A. B. Carter, A. K. Powell, R. Q. Albuquerque, A. N. Unterreiner, C. Bizzarri, *Chem. Eur. J.* **2019**, *25*, 3816–3827; m) R. Tabone, D. Feser, E. D. Lemma, U. Schepers, C. Bizzarri, *Front. Chem.* **2021**, *9*, 754420; n) A. Gusev, V. Shul'gin, E. Braga, E. Zamnius, M. Kryukova, W. Linert, *Dyes Pigm.* **2020**, *183*, 108626.

[6] a) Y. Sakai, Y. Sagara, H. Nomura, N. Nakamura, Y. Suzuki, H. Miyazaki, C. Adachi, *Chem. Commun.* **2015**, *51*, 3181–3184; b) J. Xiong, K. Li, T. Teng, X. Chang, Y. Wei, C. Wu, C. Yang, *Chem. Eur. J.* **2020**, *26*, 6887–6893; c) A. S. Berezin, K. A. Vinogradova, V. P. Krivopalov, E. B. Nikolaenkova, V. F. Plyusnin, A. S. Kupryakov, N. V. Pervukhina, D. Y. Naumov, M. B. Bushuev, *Chem. Eur. J.* **2018**, *24*, 12790–12795.

[7] T. Sano, Y. Nishio, Y. Hamada, H. Takahashi, T. Usuki, K. Shibata, *J. Mater. Chem.* **2000**, *10*, 157–161.

[8] a) X.-M. Wu, Y.-L. Hua, Z.-Q. Wang, J.-J. Zheng, X.-L. Feng, Y.-Y. Sun, *Chin. Phys. Lett.* **2005**, *22*, 1797–1799; b) M. Cibian, A. Shahalizad, F. Souissi, J. Castro, J. G. Ferreira, D. Chartrand, J.-M. Nunzi, G. S. Hanan, *Eur. J. Inorg. Chem.* **2018**, 4322–4330; c) H. Xu, R. Chen, Q. Sun, W. Lai, Q. Su, W. Huang, X. Liu, *Chem. Soc. Rev.* **2014**, *43*, 3259–3302; d) X. Li, Y. Xie, Z. Li, *Chem. Asian J.* **2021**, *16*, 2817–2829.

[9] a) J. Cepeda, E. San Sebastian, D. Padro, A. Rodríguez-Diéguez, J. A. García, J. M. Ugalde, J. M. Seco, *Chem. Commun.* **2016**, *52*, 8671–8674; b) J.-Q. Wang, Y. Mu, S.-De Han, J. Pan, J.-H. Li, G.-M. Wang, *Inorg. Chem.* **2019**, *58*, 9476–9481; c) A. Barbieri, G. Accorsi, N. Armaroli, *Chem. Commun.* **2008**, 2185–2193.

[10] Q.-D. Liu, R. Wang, S. Wang, *Dalton Trans.* **2004**, 2073–2079.

[11] a) F. A. Cotton, L. M. Daniels, P. Huang, *Inorg. Chem.* **2001**, *40*, 3576–3578; b) Y.-Y. Tang, Z.-X. Wang, P.-F. Li, Y.-M. You, A. Stroppa, R.-G. Xiong, *Inorg. Chem. Front.* **2017**, *4*, 154–159; c) X. Huang, Y. Qin, P. She, H. Meng, S. Liu, Q. Zhao, *Dalton Trans.* **2021**, *50*, 8831–8836; d) A. V. Artem'ev, M. P. Davydova, A. S. Berezin, V. K. Brel, V. P. Morgalyuk, I. Yu. Bagryanskaya, D. G. Samsonenko, *Dalton Trans.* **2019**, *48*, 16448–16456; e) M. Bortoluzzi, J. Castro, E. Trave, D. Dallan, S. Favaretto, *Inorg. Chem. Commun.* **2018**, *90*, 105–107; f) A. S. Berezin, M. P. Davydova, I. Yu. Bagryanskaya, O. I. Artyushin, V. K. Brel, A. V. Artem'ev, *Inorg. Chem. Commun.* **2019**, *107*, 107473; g) J. Chen, Q. Zhang, F.-K. Zheng, Z.-F. Liu, S.-H. Wang, A.-Q. Wu, G.-C. Guo, *Dalton Trans.* **2015**, *44*, 3289–3294; h) Y. Wu, X. Zhang, L.-J. Xu, M. Yang, Z.-N. Chen, *Inorg. Chem.* **2018**, *57*, 9175–9181; i) A. S. Berezin, D. G. Samsonenko, V.K. Brelc, A. V. Artem'ev, *Dalton Trans.* **2018**, *47*, 7306–7315; j) Y. Wu, X. Zhang, Y.-Q. Zhang, M. Yang, Z.-N. Chen, *Chem. Commun.* **2018**, *54*, 13961–13964; k) M. P. Davydova, I. A. Bauer, V. K. Brel, M. I. Rakhmanova, I. Yu. Bagryanskaya, A. V. Artem'ev, *Eur. J. Inorg. Chem.* **2020**, 695–703; l) A. V. Artem'ev, M. P. Davydova, A. S. Berezin, T. S. Sukhikh, D. G. Samsonenko, *Inorg. Chem. Front.* **2021**, *8*, 2261–2270; m) A. V. Artem'ev, M. P. Davydova, M. I. Rakhmanova, I. Yu. Bagryanskaya, D. P. Pishchur, *Inorg. Chem. Front.* **2021**, *8*, 3767–3774; n) H. Meng, W. Zhu, F. Li, X. Huang, Y. Qin, S. Liu, Y. Yang, W. Huang, Q. Zhao, *Laser Photonics Rev.* **2021**, *15*, 2100309; o) M. Bortoluzzi, J. Castro, A. Di Vera, A Palù, V. Ferraro, *New J. Chem.* **2021**, *45*, 12871–12878; p) M. Bortoluzzi, J. Castro, F. Enrichi, A. Vomiero, M. Busato, W. Huang, *Inorg. Chem. Commun.* **2018**, *92*, 145–150; q) M. Bortoluzzi, J. Castro, A. Gobbo, V. Ferraro, L. Pietrobon, S. Antoniutti, *New J. Chem.* **2020**, *44*, 571–579; r) M. Bortoluzzi, J. Castro, A. Gobbo, V. Ferraro, L. Pietrobon, *Dalton Trans.* **2020**, *49*, 7525–7534; s) M. Bortoluzzi, V. Ferraro, J. Castro, *Dalton Trans.* **2021**, *50*, 3132–3136; t) M. Bortoluzzi, J. Castro, *J. Coord. Chem.* **2019**, *72*, 309–327.

[12] a) C. A. Kosky, J. P. Gayda, J. F. Gibson, S. F. Jones, D. J. Williams, *Inorg. Chem.* **1982**, *21*, 3173–3179; b) J. P. Rose, R. A. Lalancette, J. A. Potenza, H. J. Schugar, *Acta Crystallogr. Sect. B* **1980**, *36*, 2409–2411; c) X. Liu, G. Wang, Y. Dang, S. Zhang, H. Tian, Y. Ren, X. Tao, *CrystEngComm* **2016**, *18*, 1818–1824; d) D. C. Batesky, M. J. Goldfogel, D. J. Weix, *J. Org. Chem.* **2017**, *82*, 9931–9936.

[13] L. Li, Z.-P. Wang, G.-R. Tian, X.-Y. Song, S.-X. Sun, *J. Cryst. Growth* **2008**, *310*, 1202–1205.

[14] M. W. G. de Bolster, J. F. Scholte, *Z. Anorg. Allg. Chem.* **1983**, *503*, 201–206.

[15] C. Di Iulio, M. Middleton, G. Kociok-Köhn, M. D. Jones, A. L. Johnson, *Eur. J. Inorg. Chem.* **2013**, 1541–1544.

[16] a) J. C. de Queiroz, C. Airoldi, A. P. Chagas, *J. Chem. Soc. Dalton Trans.* **1985**, 1103–1105; b) W. Grzybkowski, M. Pilarczyk, L. Klinszporn, *J. Chem. Soc. Faraday Trans. 1* **1988**, *84*, 1551–1561; c) N. Sh. Lebedeva, A. I. V'yugin, K. V. Mikhailovskii, *Russ. J. Gen. Chem.* **2003**, *73*, 968–972.

[17] a) V. Ferraro, J. Castro, E. Trave, M. Bortoluzzi, *J. Organomet. Chem.* **2022**, *957*, 122171; b) V. Ferraro, J. Castro, L. Agostinis, M. Bortoluzzi, *Transition Met. Chem.* **2021**, *46*, 391–402; c) V. Ferraro, M. Bortoluzzi, J. Castro, A. Vomiero, S. You, *Inorg. Chem. Commun.* **2020**, *116*, 107894; d) M. Bortoluzzi, J. Castro, M. Girotto, F. Enrichi, A. Vomiero, *Inorg. Chem. Commun.* **2019**, *102*, 141–146.

[18] S. P. Sinha, T. T. Pakkanen, T. A. Pakkanen, L. Niinistö, *Polyhedron* **1982**, *1*, 355–359.

[19] K. Nakamoto, *Infrared and Raman Spectra of Inorganic and Coordination Compounds, Part B: Applications in Coordination, Organometallic, and Bioinorganic Chemistry*, 6th edn, Wiley, Hoboken, New Jersey, USA **2009**, pp 120–126.

[20] Discovery Studio Visualizer 4.1. Accelrys Inc., San Diego, USA, **2014**.

[21] L. Wang, D. R. Powell, R. P. Hauser, *Dalton Trans.* **2007**, 955–964.

[22] S. C. Ward, G. Sadiq, *CrystEngComm* **2020**, *22*, 7143–7144.

[23] G. B. Deacon, J. H. S. Green, *Spectrochim. Acta Part A* **1968**, *24*, 845–852.

[24] Y. Nie, H. Pritzkow, H. Wadepohl, W. Siebert, *J. Organomet. Chem.* **2005**, *690*, 4531–4536.

[25] A. Zeller, E. Herdtweck, T. Strassner, *Acta Crystallogr. Sect. E* **2001**, *57*, m480-m482.

[26] a) X.-J. Yang, X. Liu, Y. Liu, Y. Hao, B. Wu, *Polyhedron* **2010**, *29*, 934–940; b) X. Liu, X.-J. Yang, P. Yang, Y. Liu, B. Wu, *Inorg. Chem. Commun.* **2009**, *12*, 481–483.

[27] C. Lescot, S. Savourey, P. Thuéry, G. Lefèvre, J.-C. Berthet, T. Cantat, *C. R. Chim.* **2016**, *19*, 57–70.

[28] Y. Hase, O. L. Alves, *J. Mol. Struct.* **1978**, *50*, 293–298.

[29] T. Wang, Z. Hu, X. Nie, L. Huang, M. Hui, X. Sun, G. Zhang, *Nat. Commun.* **2021**, *12*, 1364.

[30] W. L. F. Armarego, D. D. Perrin, *Purification of laboratory chemicals*, 6th edn, Butterworth-Heinemann, Oxford, UK, **2009**.

[31] M. Swiatkowski, R. Kruszynski, *Acta Crystallogr. Sect. C* **2017**, *73*, 1144–1150.

[32] M. Bortoluzzi, A. Gobbo, A. Palù, F. Enrichi, A. Vomiero, *Chem. Pap.* **2020**, *74*, 3693–3704.

[33] D. J. Pietrzyk, C. W. Frank, *Analytical Chemistry*, 2nd edn, Academic Press, New York, USA, **1979**, p. 326.

[34] Bruker, *APEX3, SMART, SAINT*, Bruker AXS Inc., Madison, Wisconsin, USA, **2015**.

[35] P. McArdle, *J. Appl. Crystallogr.* **2017**, *50*, 320–326.

[36] G. M. Sheldrick, *Acta Crystallogr. Sect. A* **2015**, 71, 3–8.

[37] G. M. Sheldrick, *Acta Crystallogr. Sect. C* **2015**, 71, 3–8.

[38] A. L. Spek, *Acta Crystallogr. Sect. E* **2020**, 76, 1–11.

[39] V. N. Staroverov, G. E. Scuseria, J. Tao, J. P. Perdew, *J. Chem. Phys.* **2003**, *119*, 12129–12137.

[40] F. Weigend, R. Ahlrichs, *Phys. Chem. Chem. Phys.* **2005**, *7*, 3297–3305.

[41] C. A. Ullrich, *Time-dependent density functional theory: Concepts and applications*, Oxford University Press, Oxford, UK, **2012**.

[42] M. J. Frisch, G. W. Trucks, H. B. Schlegel, G. E. Scuseria, M. A. Robb, J. R. Cheeseman, G. Scalmani, V. Barone, G. A. Petersson, H. Nakatsuji, X. Li, M. Caricato, A. V. Marenich, J. Bloino, B. G. Janesko, R. Gomperts, B. Mennucci, H. P. Hratchian, J. V. Ortiz, A. F. Izmaylov, J. L. Sonnenberg, D. Williams-Young, F. Ding, F. Lipparini, F. Egidi, J. Goings, B. Peng, A. Petrone, T. Henderson, D. Ranasinghe, V. G. Zakrzewski, J. Gao, N. Rega, G. Zheng, W. Liang, M. Hada, M. Ehara, K. Toyota, R. Fukuda, J. Hasegawa, M. Ishida, T. Nakajima, Y. Honda, O. Kitao, H. Nakai, T. Vreven, K. Throssell, J. A. Montgomery, Jr., J. E. Peralta, F. Ogliaro, M. J. Bearpark, J. J. Heyd, E. N. Brothers, K. N. Kudin, V. N. Staroverov, T. A. Keith, R. Kobayashi, J. Normand, K. Raghavachari, A. P. Rendell, J. C. Burant, S. S. Iyengar, J. Tomasi, M. Cossi, J. M. Millam, M. Klene, C. Adamo, R. Cammi, J. W. Ochterski, R. L. Martin, K. Morokuma, O. Farkas, J. B. Foresman, D. J. Fox, *Gaussian 16, Revision C.01*, Gaussian, Inc., Wallingford CT, USA, **2019**.

[43] T. Lu, F. Chen, *J. Comput. Chem.* **2012**, *33*, 580–592.